

1 Extensive gene duplication in 2 Arabidopsis revealed by pseudo- 3 heterozygosity

4 Benjamin Jaegle ¹, Rahul Pisupati ¹, Luz Mayela Soto-Jiménez ¹, Robin Burns ^{1 3}, Fernando A.
5 Rabanal ², Magnus Nordborg ¹

6 Abstract

7 **Background:** It is apparent that genomes harbor massive amounts of structural variation, and
8 that this variation has largely gone undetected for technical reasons. In addition to being
9 inherently interesting, structural variation can cause artifacts when short-read sequencing data
10 are mapped to a reference genome. In particular, spurious SNPs (that do not show Mendelian
11 segregation) may result from mapping of reads to duplicated regions. Calling SNP using the raw
12 reads of the 1001 Arabidopsis Genomes Project we identified 3.3 million heterozygous SNPs
13 (44% of total). Given that *Arabidopsis thaliana* (*A. thaliana*) is highly selfing, we hypothesized
14 that these SNPs reflected cryptic copy number variation, and investigated them further.

15 **Results:** The heterozygosity we observed consisted of particular SNPs being heterozygous
16 across individuals in a manner that strongly suggests it reflects shared segregating duplications
17 rather than random tracts of residual heterozygosity due to occasional outcrossing. Focusing on
18 such pseudo-heterozygosity in annotated genes, we used GWAS to map the position of the
19 duplicates, identifying 2500 putatively duplicated genes. The results were validated using *de*
20 *novo* genome assemblies from six lines. Specific examples included an annotated gene and
21 nearby transposon that, in fact, transpose together. Finally, we use existing bisulfite sequencing
22 data to demonstrate that cryptic structural variation can produce highly inaccurate estimates of
23 DNA methylation polymorphism.

24 **Conclusions:** Our study confirms that most heterozygous SNPs calls in *A. thaliana* are
25 artifacts, and suggest that great caution is needed when analyzing SNP data from short-read
26 sequencing. The finding that 10% of annotated genes exhibit copy-number variation, and the

27 realization that neither gene- nor transposon-annotation necessarily tells us what is actually
28 mobile in the genome suggest that future analyses based on independently assembled
29 genomes will be very informative.

30 **Keywords:** structural variation, gene duplication, GWAS, SNP calling, methylation

31 Introduction

32 With the sequencing of genomes becoming routine, it is evident that structural variants (SVs)
33 play a major role in genome variation (Alkan, Coe, and Eichler 2011). There are many kinds of
34 SVs, e.g., indels, inversions, and transpositions. Of particular interest from a functional point of
35 view is gene duplication, leading to copy number variation (CNV).

36 Before Next-Generation Sequencing (NGS) was available, genome-wide detection of CNVs
37 was achieved using DNA-microarrays. These methods had severe weaknesses, leading to low
38 resolution and problems detecting novel and rare mutations. (Carter 2007; Snijders et al. 2001).
39 With the development of NGS, our ability to detect CNVs increased dramatically, using tools
40 based on split reads, paired-end mapping sequencing coverage, or even *de novo* assembly
41 (Shendure and Ji 2008; Zhao et al. 2013). In mammals, many examples of CNVs with a major
42 phenotypic effect have been found (Gonzalez et al. 2005; Perry et al. 2007; Handsaker et al.
43 2011). One example is the duplication of MWS/MLS, associated with better trichromatic color
44 vision (Miyahara et al. 1998).

45 While early investigation of CNV focused on mammals, several subsequent studies have
46 looked at plant genomes. In *Brassica rapa*, gene CNV has been shown to be involved in
47 morphological variation (Lin et al. 2014) and an analysis of the poplar “pan-genome” revealed at
48 least 3000 genes affected by CNV (Pinosio et al. 2016). It has also been shown that variable
49 regions in the rice genome are enriched in genes related to defense to biotic stress. (Yao et al.
50 2015). More recently, the first chromosome-level assemblies of seven accessions of *A. thaliana*
51 based on long-read sequencing were released (Jiao and Schneeberger 2019), demonstrating
52 that a large proportion of the genome is structurally variable. Similar studies have also been
53 carried out in maize (C. Li et al. 2020; Hufford et al. 2021), tomato (Alonge et al. 2020), rice
54 (Zhou et al. 2020) and soybean (Y. Liu et al. 2020). These approaches are likely to provide a
55 more comprehensive picture than short-read sequencing, but are also far more expensive.

56 In 2016, the 1001 Genomes Consortium released short-read sequencing data and SNP
57 calls for 1135 *A. thaliana* accessions (1001 Genomes Consortium 2016). Several groups have

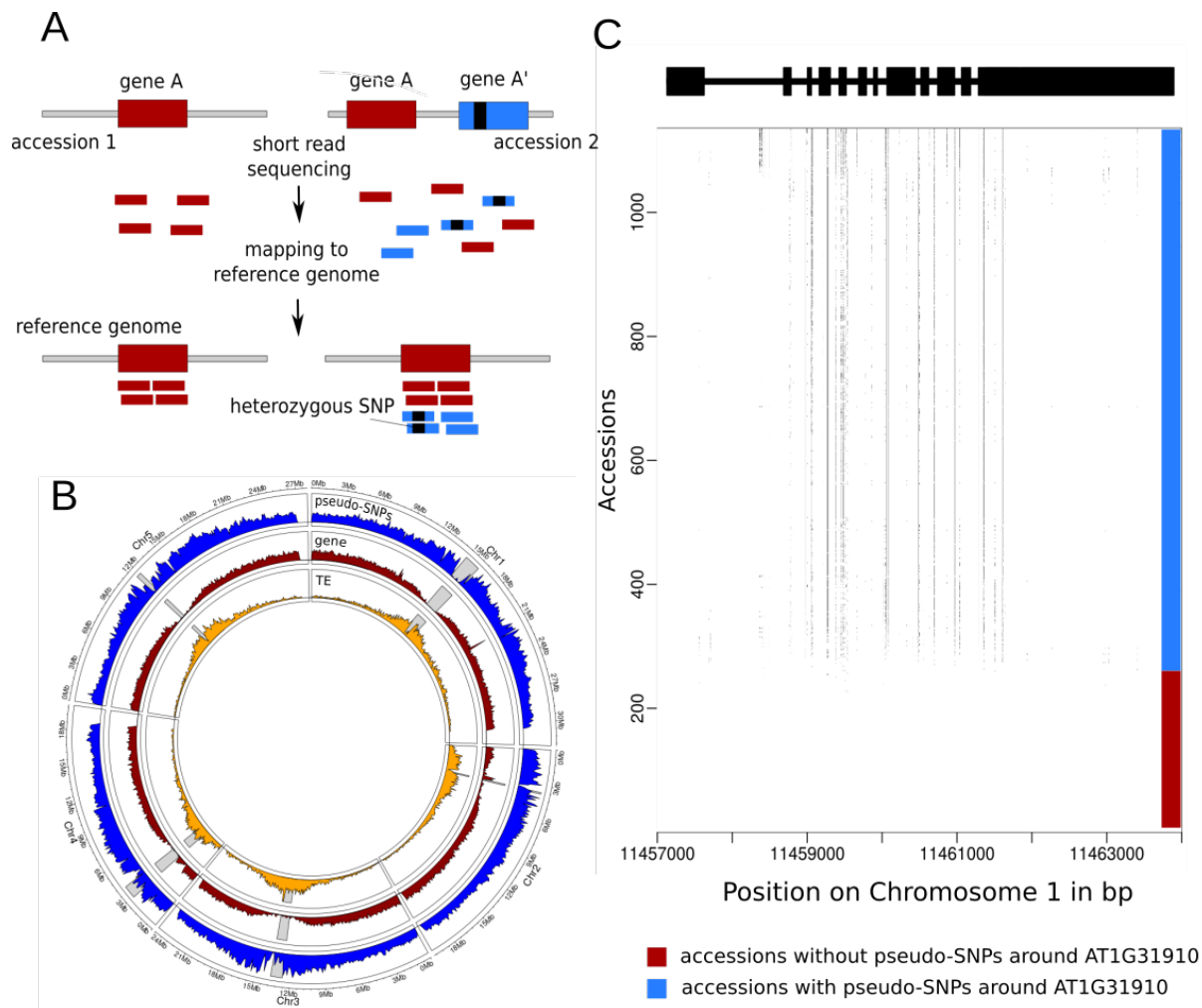
58 used these data to identify large numbers of structural variants using split reads (Göktay,
59 Fulgione, and Hancock 2020; Zmienko et al. 2020; D.-X. Liu et al. 2021). Here we approach this
60 from a different angle. Our starting point is the startling observation that, when calling SNPs in
61 the 1001 Genomes data set, we identified 3.3 million (44% of total) putatively heterozygous
62 SNPs. In a highly selfing organism, this is obviously highly implausible, and these SNPs were
63 flagged as spurious: presumably products of cryptic CNV, which can generate “pseudo-SNPs”
64 (Ranade et al. 2001; Hurlles 2002) when sequencing reads from non-identical duplicates are
65 (mis-)mapped to a reference genome that does not contain the duplication. Note that allelic SNP
66 differences are expected to exist *ab initio* in the population, leading to instant pseudo-
67 heterozygosity as soon as the duplicated copy recombines away from its template. In this paper
68 we return to these putative pseudo-SNPs and show that they are indeed largely due to
69 duplications, the position of which can be precisely mapped using GWAS. Our approach is
70 broadly applicable, and we demonstrate that it can reveal interesting biology.

71 Results

72 Massive pseudo-heterozygosity in the 1001 Genomes data

73 Given that *A. thaliana* is highly selfing, a large fraction (44%) of heterozygous SNPs is
74 inherently implausible. Two other lines of evidence support the conclusion that they are
75 spurious. First, genuine residual heterozygosity would appear as large genomic tracts of
76 heterozygosity in individuals with recent outcrossing in their ancestry. Being simply a random
77 product of recombination and Mendelian segregation, there is no reason two individuals would
78 share tracts unless they are very closely related. The observed pattern is completely the
79 opposite. While a small number of individuals do show signs of recent outcrossing, this is quite
80 rare (as expected given the low rate of outcrossing in this species, and the fact that the
81 sequenced individuals were selected to be completely inbred). Instead we find that the same
82 SNP are often heterozygous in multiple individuals. Although the population level of
83 heterozygosity at a given SNP is typically low (**Supplemental Figure 1**), over a million
84 heterozygous SNPs are shared by at least 5 accessions, and a closer look at the pattern of
85 putative heterozygosity usually reveals short tracts of shared heterozygosity that would be
86 vanishingly unlikely under residual heterozygosity, but would be expected if tracts represent
87 shared duplications, and heterozygosity is, in fact, pseudo-heterozygosity due to mis-mapped

88 reads (**Figure 1**). Analysis of the distribution of the lengths and number of putatively
 89 heterozygous tracts across accessions shows that the vast majority of accessions have a large
 90 number of very short tracts (roughly 1 kb) of heterozygosity (**Supplemental Figure 2**). Longer
 91 tracts are rare and not shared between accessions.



92 **Figure 1:** Pseudo-heterozygosity in the 1001 Genomes dataset. **(A)** Cartoon illustrating how a duplication
 93 can generate pseudo-SNPs when mapping to a reference genome that does not contain the duplication.
 94 **(B)** Genomic density of transposons, genes, and shared heterozygous SNPs. Gray bars represent the
 95 position of the centromere for each chromosome. **(C)** The pattern of putative heterozygosity around
 96 AT1G31910 for the 1057 accessions. Dots in the plot represent putative heterozygosity.

97 Furthermore, the density of shared heterozygous SNPs is considerably higher around the
 98 centromeres (**Figure 1**), which is again not expected under random residual heterozygosity, but
 99 is rather reminiscent of the pattern observed for transposons, where it is interpreted as the
 100 result of selection removing insertions from euchromatic regions, leading to a build-up of

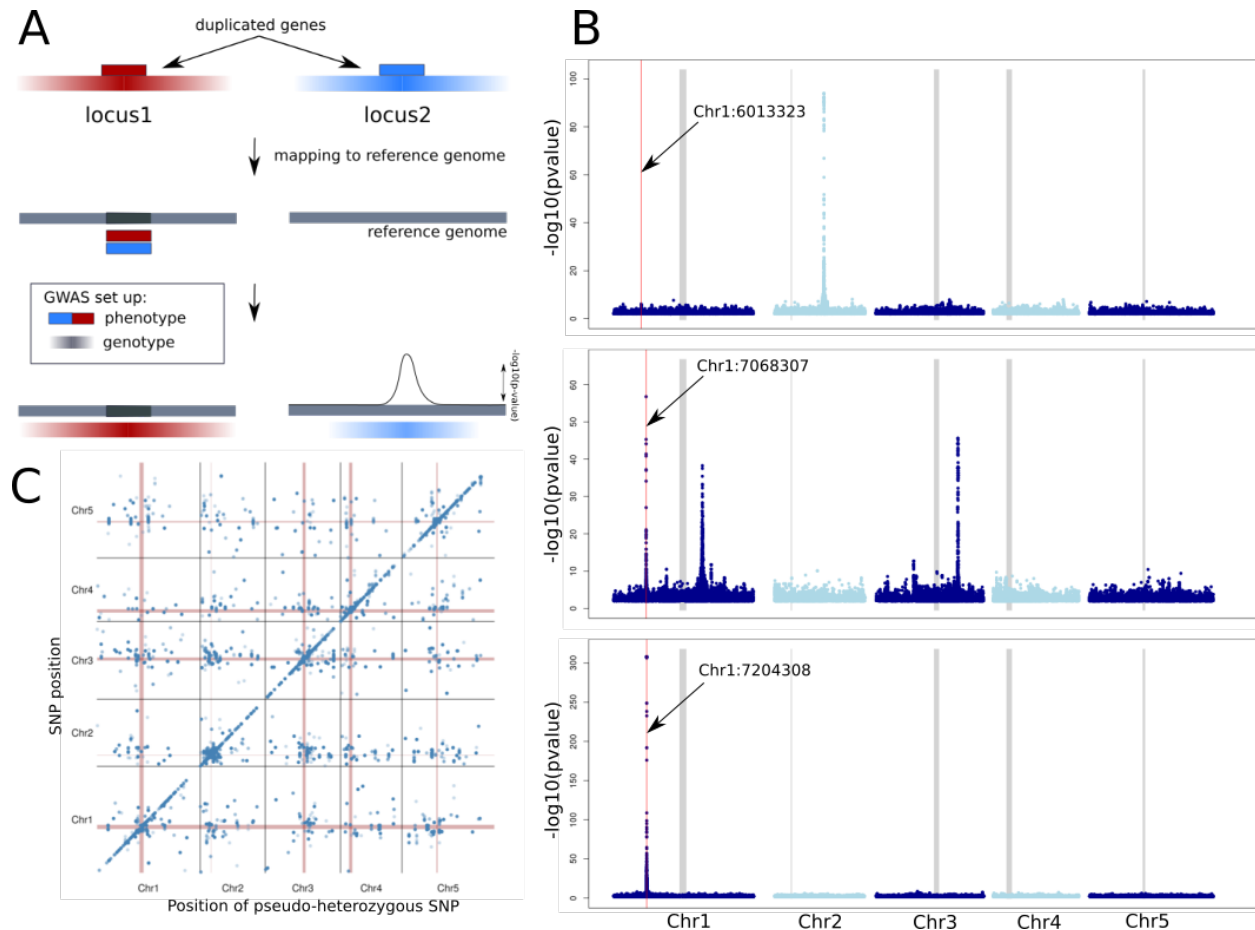
101 common (shared) transposon insertions near centromere (Quadrana et al. 2016). As we shall
102 see below, it is likely that transposons play an important role in generating cryptic duplications
103 leading to pseudo-heterozygosity (although we emphasize again that the heterozygous SNPs
104 were called taking known repetitive sequences into account).

105 Despite the evidence for selection against these putative duplications, we found 2570 genes
106 containing 26647 pseudo-SNPs segregating at 5% or more in the population (**Supplemental**
107 **Figure 3**). Gene-ontology analysis of these genes reveals an enrichment for biological
108 processes involved in response to UV-B, bacteria or fungi (**Supplemental Figure 4**). In the
109 following sections, we investigate these putatively duplicated genes further.

110 Mapping common duplications using genome-wide association

111 If heterozygosity is caused by the presence of cryptic duplications in non-reference genomes, it
112 should be possible to map the latter using GWAS with heterozygosity as a “phenotype”
113 (Imprialou et al 2017). We did this for each of the 26647 SNPs exhibiting shared heterozygosity
114 within genes (**Supplemental Figure 3**).

115 Of the 2570 genes that showed evidence of duplication, 2511 contained at least one major
116 association (using significance threshold of $p < 10^{-20}$; see Methods). For 708 genes, the
117 association was more than 50 kb away from the pseudo-SNP used to define the phenotype, and
118 for 175 it was within 50 kb. We will refer to these as *trans*- and *cis*-associations, respectively.
119 The majority of genes, 1628, had both *cis*- and *trans*-associations (**Figure 2**).



120 **Figure 2:** GWAS of putative duplications **(A)** Schematic representation of the principle of how GWAS can
 121 be used to detect the position of the duplicated genes based on linkage disequilibrium (LD). As
 122 phenotype, heterozygosity at the position of interest is coded as 1 (present) or 0 (absent). As genotype,
 123 the SNPs matrix of the 1001 genome dataset was used (with heterozygous SNPs filtered out). Color
 124 gradients represent the strength of LD around the two loci. In this example the reference genome does
 125 not contain locus2. **(B)** GWAS results for three different genes with evidence of duplication, for illustration.
 126 The red lines indicate the position of the pseudo-SNP used for each gene/GWAS and the thick grey lines
 127 indicate the centromeres. The top plot shows a *trans*-association, the bottom a *cis*-association, and the
 128 middle shows a case with both (*cis* plus two *trans*). **(C)** Summary of all 26647 GWAS results.

129 To validate these results, we assembled 6 non-reference genomes *de novo* using long-read
 130 PacBio sequencing. The GWAS results provide predicted locations of the duplications (the
 131 putative causes of pseudo-heterozygosity). We identified the homologous region of each non-
 132 reference genome, then used BLAST to search for evidence of duplication. For 84% of the 403
 133 genes predicted to have a duplication present in at least one of the six non-reference genomes,
 134 evidence of a duplication was found; for 60%, the occurrence perfectly matched the pattern of

135 heterozygosity across the six genomes. For the remaining 16%, no evidence of a duplication
136 was found, which could be due to the stringent criteria we used to search for evidence of
137 duplication (see Methods). The distribution of fragment sizes detected suggests that we capture
138 a mixture of duplicated gene fragments and full genes (**Supplemental Figure 5**).

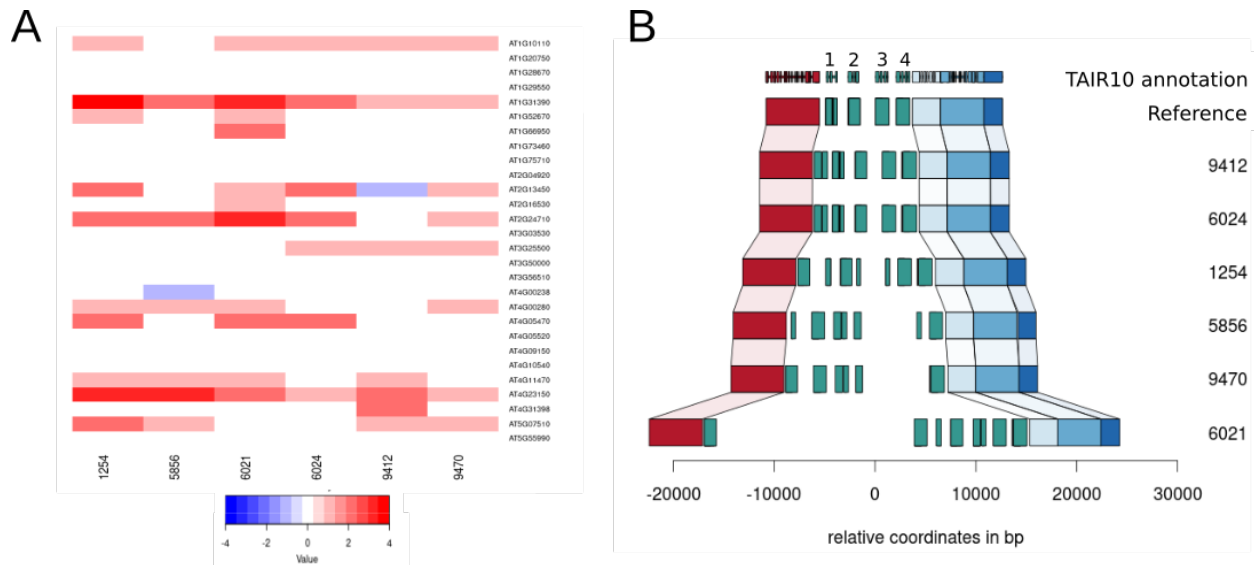
139 Rare duplications

140 The GWAS approach has no power to detect rare duplications, which is why we restricted the
141 analysis above to pseudo-heterozygous SNPs seen in five or more individuals. Yet most are
142 rarer: 40% are seen only in a single individual, and 16% are seen in two. As it turns out, many of
143 these appear to be associated with more common duplications. Restricting ourselves to genes
144 only, 11.4% of the singleton pseudo-heterozygous SNPs are found in the 2570 genes already
145 identified using common duplications, a significant excess ($p = 2.5e-109$). For doubletons, the
146 percentage is 11.1% ($p = 1.9e-139$). Whether they are caused by the same duplications, or
147 reflect additional ones present at lower frequency is difficult to say. To confirm duplications more
148 directly, we took the reads generating the singleton and doubleton pseudo-heterozygotes, and
149 compared the result of mapping them to the reference genome, and to the appropriate genome
150 (derived from the same inbred line). One predicted consequence of the reads mapping at
151 different locations is that mapping coverage around the pseudo-SNPs will be decreased when
152 mapping to the newly assembled PacBio genomes rather than the reference genome. As
153 expected, a high proportion of the SNPs tested have lower coverage when mapping to the
154 PacBio genomes (**Supplemental Figure 6-7**). In addition to a decrease in coverage, we were
155 also able to detect reads mapping to multiple locations in the right genomes, as well as the
156 corresponding disappearance of the pseudo-SNPs. For example, 41.5% of the doubletons tag
157 regions that map to more regions in the PacBio genomes than in the reference genome
158 (**Supplemental Figure 6-8**).

159 Local duplications

160 If duplications arise via tandem duplications, they will not give rise to pseudo-SNPs until the
161 copies have diverged via mutations. This is in contrast to unlinked copies, which will lead to
162 pseudo-SNPs due to existing allelic variation as soon as recombination has separated copy
163 from original. We should thus expect the approach taken here to be biased against detecting
164 local duplications. Nonetheless, GWAS revealed 175 genes with evidence only for a *cis*
165 duplication. 28 of these were predicted to be present in at least one of the six new genomes,

166 and 14 could be confirmed to have local variation of copy number relative to the reference.
 167 **(Figure 3A).**



168 **Figure 3:** Confirmation of tandem duplications. **(A)** The distribution of estimated copy number (based on
 169 sequencing coverage) across 6 PacBio genomes for 28 genes predicted to be involved in tandem
 170 duplications based on the analyses of this paper. **(B)** The duplication pattern observed in these genomes
 171 for the gene AT1G31390, as an example. The reference genome contains four copies, shown as
 172 numbered green boxes. Other colored boxes denote other genes.

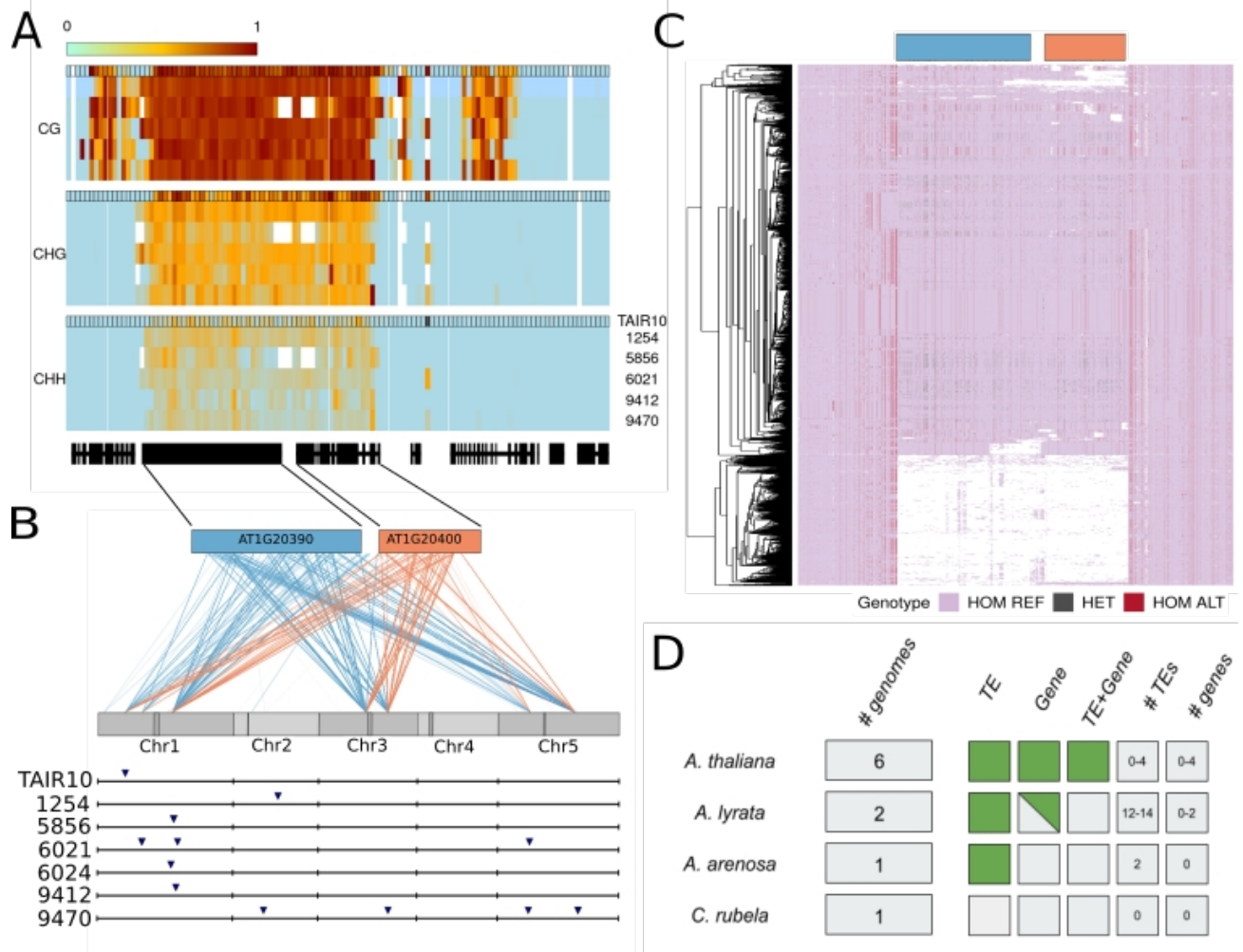
173 The local structure of the duplications can be complex. An example is provided by the gene
 174 AT1G31390, annotated as a member of MATH/TRAF-domain genes, and which appears to be
 175 present in 4 tandem copies in the reference genome, but which is highly variable between
 176 accessions, with one of our accessions carrying at least 6 copies (**Figure 3B**). However, there
 177 are no copies elsewhere in any of the new genomes for this gene (**Supplemental Figure 9**).

178 Transposon-driven duplications

179 Transposons are thought to play a major role in gene duplications, capturing and moving genes
 180 or gene fragments around the genome (Woodhouse, Pedersen, and Freeling 2010; Lisch 2013).
 181 While confirming the *trans* duplications in the PacBio genomes, we found a beautiful example of
 182 this process. The gene AT1G20400 (annotated, based on sequence similarity, to encode a
 183 myosin heavy chain-like protein) was predicted to have multiple *trans*-duplications. The 944 bp
 184 coding region contains 125 putatively heterozygous SNPs with striking haplotype structure
 185 characteristic of structural variation (**Figure 4C**). We were able to identify the duplication
 186 predicted by GWAS in the six new genomes (**Figure 4**). Four of the newly assembled genomes

187 have only one copy of the gene, just like the reference genome, but one has 3 copies and one
188 has 4 copies. However, none of the 6 new genomes has a copy in the same place as in the
189 reference genome (**Supplemental Figure 10**).

190 In the reference genome, AT1G20400 is closely linked to AT1G20390, which is annotated
191 as a Gypsy element. This element also contains many pseudo-SNPs, and GWAS revealed
192 duplication sites overlapping those for AT1G20400 (**Figure 4B**). This suggested that the
193 putative gene and putative Gypsy element transpose together, i.e. that both are misannotated,
194 and that the whole construct is effectively a large transposable element. Further analysis of the
195 PacBio genomes confirmed that AT1G20400 and AT1G20390 were always found together, and
196 we were also able to find conserved Long Terminal Repeat sequences flanking the whole
197 construct, as would be expected for a retrotransposon (**Supplemental Figure 11-12**). We did
198 not find any evidence for expression of AT1G20400 in RNAseq from seedlings in any of the
199 accessions. Available bisulfite sequencing data (Kawakatsu et al. 2016) showed that the whole
200 region is heavily methylated, as expected for a transposon (**Figure 4**). We tried mapping the
201 bisulfite reads to the appropriate genome for the respective accessions, but the coverage was
202 too low and noisy to observe a difference in methylation between the multiple insertions
203 (**Supplemental Figure 13**).



204 **Figure 4:** A Gypsy element (AT1G20390) and a gene transposon (AT1G20400) together. **(A)** Methylation
 205 levels on regions containing AT1G20390 and AT1G20400 for 6 accessions, calculated in 200 bp windows
 206 after mapping reads to the TAIR10 reference genome (annotation outline in black). **(B)** GWAS results for
 207 the putatively heterozygous SNPs in AT1G20390 and AT1G20400. Each line represents the link between
 208 the position of the pseudo-SNP and a GWAS hit position in the genome. The lower part shows the
 209 presence of the new transposable element in the 6 PacBio genomes as well as in the reference genome.
 210 **(C)** SNP haplotypes around the AT1G20400 region in the 1001 genomes data. White represents a lack of
 211 coverage. **(D)** Presence of the gene and the transposon in related species.

212 Having located precise insertions in the six new genomes, we attempted to find them using
 213 short-read data in the 1001 Genomes dataset. Except for one insertion that was shared by 60%
 214 of accessions, the rest were found in less than 20%, suggesting that this new element has no
 215 fixed insertions in the genome — including the insertion found in the TAIR10 reference genome,
 216 which was only found in 17.4 % of the accessions (**Supplemental Figure 14**). We also looked
 217 for the element in the genomes of *A. lyrata* (two different genomes), *A. suecica* (a tetraploid

218 containing an *A. thaliana* and an *A. arenosa* subgenome; see Burns et al. 2021), and *Capsella*
219 *rubella* (Slotte et al. 2013). The gene and the Gypsy element were only found together in *A.*
220 *thaliana* (including the *A. thaliana* sub-genome of the allopolyploid *A. suecica*). The Gypsy
221 element alone is present in the other *Arabidopsis* species, and the gene alone is present in *A.*
222 *lyrata*, but only in one of two genomes. In *Capsella rubella*, neither the transposon nor the gene
223 could be detected (**Supplemental Figure 15**). Thus the transposon and gene appears to be
224 specific to the genus *Arabidopsis*, while their co-transposition is specific to *A. thaliana*,
225 suggesting that the new transposable element evolved since divergence of *A. thaliana* from the
226 other member of the genus.

227 Spurious methylation polymorphism

228 Just like cryptic duplications can lead to spurious genetic polymorphisms, they can lead to
229 spurious cytosine methylation polymorphisms. Indeed, given the well-established connection
230 between gene duplication and gene silencing (e.g., Melquist, Luff, and Bender 1999), they may
231 be more likely to do so. To investigate this, we re-examined the methylation status of genes
232 previously reported by the 1001 Genomes Project (Kawakatsu et al. 2016) as having complex
233 patterns of methylation involving both CG and CHG methylation. In our six sequenced
234 accessions, we found 19530 genes that had been reported as having CG methylation (in at
235 least one accession) and 2556 genes that had been reported as having CHG methylation (in at
236 least one accession). 2473 genes were part of both sets. Out of these, 619, or 24%, had been
237 detected as duplicated in the analyses presented above (a massive enrichment compared to the
238 genome-wide fraction of roughly 10%). To understand these patterns better, we mapped the
239 original bisulfite data to the appropriate genome as well as to the reference genome. In any
240 given accession, roughly 7% of the 2473 genes could not be compared because the
241 homologous copy could not be found (this is presumably mostly because they contain structural
242 variants that prevent them being located by BLAST; see Supplementary Table 1), and roughly
243 30% exhibited copy number variation (Table 1). The remaining genes had a single match,
244 almost always in the same location as in the reference genome. These categories are shared
245 across accessions: 1294 of the 2367 genes appeared to be single-copy in all six new genomes,
246 for example (Table 1; Additional files 1-8).

247 Turning to the methylation patterns, the effect of cryptic copy number variation was obvious
248 (Table 2). For the genes with a single match in both the reference and accession genome,
249 methylation status calls based on mapping bisulfite sequencing reads to either genome were

250 largely concordant (roughly 2.5% disagreement), whereas for genes with copy number variation,
251 roughly one third of calls were wrong.

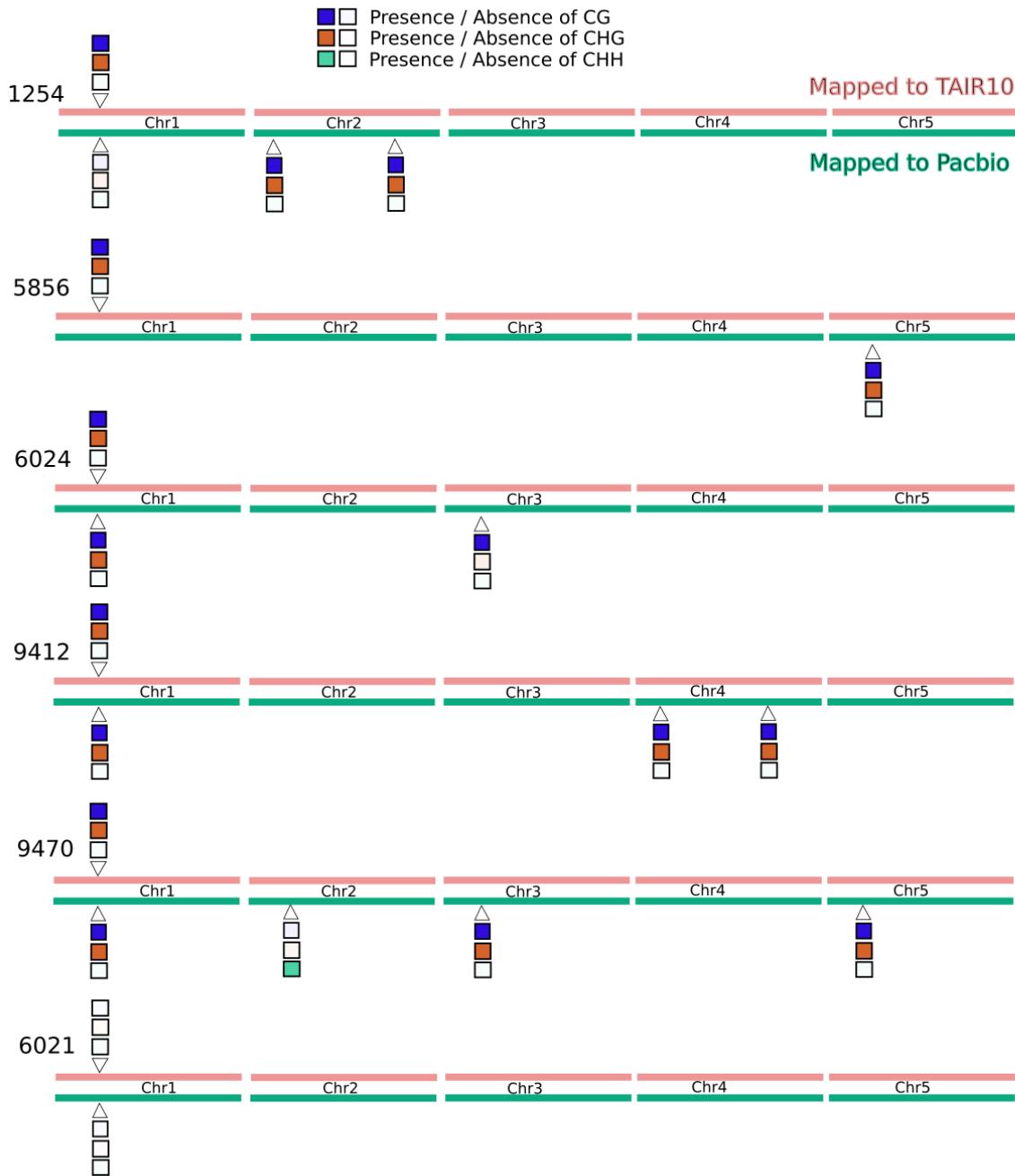
252 Table 1. Number of copies of the 2367 genes identified in each new genome (and Araport11, as control).

Target	Number of copies identified		
	0	1	>1
1254	138	1563	772
5856	174	1566	733
6021	131	1577	765
6024	152	1554	767
9412	147	1567	759
9470	142	1589	742
<i>Intersection</i>	37	1294	610
Araport11	0	1721	752

253 **Table 2.** Fraction of differentially methylated genes when comparing bisulfite reads mapped to reference
254 TAIR genome and to its respective PacBio genome, separated by gene copy number.

Target	Number of copies identified			
	1		>1	
	CG (%)	CHG (%)	CG (%)	CHG (%)
1254	3.0	4.4	33.3	21.6
5856	1.2	3.7	27.8	42.9
6021	2.4	3.2	39.3	24.2
6024	3.0	4.2	41.2	29.5
9412	2.0	2.5	37.0	27.1
9470	2.1	4.7	36.0	26.2

255 As an illustration for why this occurs, consider the methylation status of AT1G30140 (**Figure**
256 **5**). When mapped to the reference genome, 5 out of 6 accessions were found to be both CG
257 and CHG methylated, with accession 6021 having no methylation. When mapped to the
258 appropriate genome, we see that this pattern can be quite misleading. In accession 1254, for
259 example, we found three apparent copies of the gene, only two of which are methylated, neither
260 of which is the copy corresponding to the copy present in the reference genome. In accession
261 5856, the copy corresponding to the reference genome cannot be identified, but a copy on a
262 different chromosome is identified, and it is methylated. In both cases, mapping to the reference
263 genome leads to incorrect methylation status for AT1G30140.



264 **Figure 5:** The effect of calling methylation status for AT1G30140 by mapping to a reference genome vs.
265 the appropriate genome. Locations on the chromosomes are approximate, for illustration only.

266 Discussion

267 A duplication can lead to pseudo-SNPs when SNPs are identified by mapping short reads to a
268 reference genome that does not contain the duplication. Typically pseudo-SNPs have to be
269 identified using non-Mendelian segregation patterns in families or crosses, but in inbred lines
270 they can be identified solely by their presence. The overwhelming majority of the 3.3 million
271 heterozygous SNPs (44% of total) identified by our SNP-calling of the 1001 Genomes Project
272 (2016) data are likely to be pseudo-SNPs. Assuming this, we used (pseudo-)heterozygosity as a
273 “phenotype”, and tried to map its cause, i.e. the duplication, using a simple but powerful GWAS
274 approach. Focusing on annotated genes, we find that over 2500 (roughly 10% of total) harbor
275 pseudo-SNPs and show evidence of duplication. Using 6 new long-read assemblies, we were
276 able to confirm 60% of these duplications using conservative criteria (see Methods). Most of the
277 remaining duplications are located in pericentromeric regions where SNP-calling has lower
278 quality, and which are difficult to assemble even with long-read (**Supplemental Figure 16**).

279 These numbers nearly certainly underestimate the true extent of duplication, which has
280 been known to be common in *A. thaliana* for over a decade (Cao et al. 2011; Gan et al. 2011;
281 Schneeberger et al. 2011). While unlinked *trans*-duplications are fairly likely to give rise to
282 pseudo-SNPs, local *cis*-duplications will only do so once sufficient time has passed for
283 substantial sequence divergence to occur, or if they arise via non-homologous recombination in
284 a heterozygous individual (which is less likely in *A. thaliana*). As for the GWAS approach, it
285 lacks statistical power to detect rare duplications, and can be misled by allelic heterogeneity
286 (due to multiple independent duplications). Finally, duplications are just a subset of structural
287 variants, and it is therefore not surprising that other short-read approaches to detect such
288 variants have identified many more using the 1001 Genomes data (Zmienko et al. 2020; D.-X.
289 Liu et al. 2021; Göktay, Fulgione, and Hancock 2020).

290 Pseudo-SNPs is not the only problem with relying on a reference genome. Our analysis
291 uncovered a striking example of the potential importance of the “mobileome” in shaping genome
292 diversity (Morgante et al. 2005): we show that an annotated gene and an annotated transposon
293 are both part of a much larger mobile element, and the insertion in the reference genome is
294 missing from most other accessions. When short reads from another accession are mapped to
295 this “gene” using the reference genome, you are neither mapping to a gene, nor to the position

296 you think. One possible consequence of this is incorrect methylation polymorphism calls, as we
297 demonstrate above, but essentially any methodology that relies on mapping sequencing data to
298 a reference genome could be affected (e.g. RNA-seq).

299 Time (and more independently assembled genomes) will tell how significant this problem is,
300 but the potential for artifactual results is clearly substantial, and likely depends on the amount of
301 recent transposon activity (Morgante et al. 2005). It is also important to realize that the
302 artefactual nature of the 44% heterozygous SNPs was only apparent because we are working
303 with inbred lines. Other researchers working on inbred lines have reached similar conclusions,
304 and used various methods to eliminate them e.g. *Zea* (Chia et al. 2012; Lu et al. 2015;
305 Bukowski et al. 2018) and *Brachypodium* (Stritt et al. 2021). In human genetics, SNP-calling
306 relies heavily on family trios, but in outcrossing organisms where this is not possible, there is
307 great cause for concern. The increasing ease and ability to sequence more and more complex
308 genomes, such as projects associated with the 1001G+ and Tree of Life, will allow population
309 analyses to avoid the use of a single reference genome and reveal new mechanisms of gene
310 duplication and structural variants such as those reported here.

311 Methods

312 Long-read sequencing of six *A. thaliana*

313 We sequenced six Swedish *A. thaliana* lines that are part of the 1001 Genomes collection (1001
314 Genomes Consortium 2016), ecotype ids: 1254, 5856, 6021, 6024, 9412 and 9470. Plants were
315 grown in the growth chamber at 21 C in long-day settings for 3 weeks and dark-treated for 24-
316 48 hours before being collected. DNA was extracted from ~20 g of frozen whole seedling
317 material following a high molecular weight DNA extraction protocol adapted for plant tissue
318 (Cristina Barragan et al. 2021). All six genomes were sequenced with PacBio technology, 6021
319 with PacBio RSII, and the rest with Sequel. Accession 9412 was sequenced twice and 6024
320 was additionally sequenced with Nanopore (4.1 Gbp sequenced, 376 K reads with N50 18.7
321 Kb). All data were used in the assemblies.

322 MinION sequencing of two *A. lyrata*

323 We sequenced two North American *A. lyrata* accessions, 11B02 and 11B21. Both individuals
324 come from the 11B population of *A. lyrata*, which is self-compatible and located in Missouri
325 (Griffin and Willi 2014) (GPS coordinates 38° 28' 07.1" N; 90° 42' 34.3" W) . Plants were bulked
326 for 1 generation in the lab and DNA was extracted from ~20g of 3-week old seedlings, grown at
327 21°C and dark treated for 3 days prior to tissue collection. DNA was extracted using a modified
328 protocol for high molecular-weight DNA extraction from plant tissue. DNA quality was assessed
329 with a Qubit fluorometer and a Nanodrop analysis. We used a Spot-ON Flow Cell FLO-
330 MIN106D R9 Version with a ligation sequencing kit SQK-LSK109. Bases were called using
331 guppy version 3.2.6 (<https://nanoporetech.com/community>). The final output of MinION
332 sequencing for 11B02 was 13,67 Gbp in 763,800 reads and an N50 of 31,15 Kb. The final
333 output of MinION sequencing for 11B21 was 17.55 Gb, 1.11 M reads with an N50 of 33.26 Kb.

334 Genome assembly, polishing and scaffolding

335 The six *A. thaliana* genomes (ecotype ids 1254, 5856, 6021, 6024, 9412 and 9470) were
336 assembled using Canu (v 1.7.1) (Koren et al. 2017) with default settings, except for
337 genomeSize. Previous estimates of flow cytometry were used for this parameter (Long et al.
338 2013) when available or 170m was used. The values were 170m, 178m, 135m, 170m, 170m
339 and 170m, respectively. The assemblies were corrected with two rounds of arrow (PacBio's
340 SMRT Link software release 5.0.0.6792) and one of Pilon (Walker et al. 2014). For arrow, the
341 respective long reads were used and for Pilon, the 1001 Genomes DNA sequencing data, plus
342 PCR-free Illumina 150bp data that was generated for accessions 6024 and 9412; lines 5856,
343 6021, 9470 had available PCR-free data (250bp reads generated by David Jaffe, Broad
344 Institute). This resulted in 125.6Mb, 124.3Mb, 124.5Mb, 124.7Mb, 127.1Mb and 128Mb
345 assembled bases, respectively; contained in 99, 436, 178, 99, 109 and 124 contigs,
346 respectively. The polished contigs were ordered and scaffolded with respect to the Col-0
347 reference genome, using RaGOO (Alonge et al. 2019).

348 We assembled the genome of the two *A. lyrata* accessions 11B02 and 11B21 using Canu
349 (Koren et al. 2017) (v 1.8) with default settings and a genome size set to 200Mb. The genomes
350 of 11B02 and 11B21 were contained in 498 and 265 contigs, respectively. The contig
351 assemblies were polished using Racon (Vaser et al. 2017) (v 1.4) and ONT long reads were
352 mapped using ngmlr (Sedlazeck et al. 2018) (v 0.2.7). Assemblies were further polished by
353 mapping PCR-free Illumina 150bp short reads (~100X for 11B02 and ~88X for 11B21) to the

354 long-read corrected assemblies. Short-read correction of assembly errors was carried out using
355 Pilon (Walker et al. 2014) (v1.23). Contigs were scaffolded into pseudo-chromosomes using
356 RaGOO (Alonge et al. 2019) and by using the error corrected long reads from Canu and the *A.*
357 *lyrata* reference genome (Hu et al. 2011) and the *A. arenosa* subgenome of *A. suecica* (Burns
358 et al. 2021) as a guide followed by manual inspection of regions. The assembly size for 11B02
359 was 213Mb and 11B21 was 202Mb. Genome size was estimated using findGSE (Sun et al.
360 2018) with a resulting estimated genome size of ~256Mb for 11B02 and ~237Mb for 11B21.

361 Heterozygous SNPs calling / extraction

362 We downloaded short-read data for 1,057 accessions from the 1001 Genomes Project (1001
363 Genomes Consortium 2016). Raw paired-end reads were processed with cutadapt (v1.9)
364 (Martin 2011) to remove 3' adapters, and to trim 5'-ends with quality 15 and 3'-ends with quality
365 10 or N-endings. All reads were aligned to the *A. thaliana* TAIR10 reference genome
366 (Arabidopsis Genome Initiative 2000) with BWA-MEM (v0.7.8) (H. Li 2013), and both Samtools
367 (v0.1.18) and Sambamba (v0.6.3) were used for various file format conversions, sorting and
368 indexing (H. Li et al. 2009; Tarasov et al. 2015), while duplicated reads were by marked by
369 Markduplicates from Picard (v1.101; <http://broadinstitute.github.io/picard/>). Further steps were
370 carried out with GATK (v3.4) functions (Van der Auwera et al. 2013; DePristo et al. 2011). Local
371 realignment around indels were done with 'RealignerTargetCreator' and 'IndelRealigner', and
372 base recalibration with 'BaseRecalibrator' by providing known indels and SNPS from The 1001
373 Genomes Consortium (1001 Genomes Consortium 2016). Genetic variants were called with
374 'HaplotypeCaller' in individual samples followed by joint genotyping of a single cohort with
375 'GenotypeGVCFs'. An initial SNP filtering was done following the variant quality score
376 recalibration (VQSR) protocol. Briefly, a subset of ~181,000 high quality SNPs from the RegMap
377 panel (Horton et al. 2012) were used as the training set for VariantRecalibrator with a priori
378 probability of 15 and four maximum Gaussian distributions. Finally, only bi-allelic SNPs within at
379 a sensitivity tranche level of 99.5 were kept, for a total of 7,311,237 SNPs.

380 Heterozygous stretches analysis

381 From the VCF, Plink was used to generate .ped and .map files.
382 (<http://pngu.mgh.harvard.edu/purcell/plink/>) (Purcell et al. 2007). To detect and characterize the
383 stretches of heterozygosity the package "detectRUNS" in R was then used.
384 (<https://github.com/bioinformatics-ptp/detectRUNS/tree/master/detectRUNS>). We used the

385 function slidingRuns.run with the following parameters: WindowSize=10, threshold=0.05,
386 RoHet=True, minDensity=1/100, rest as default.

387 SNP filtering

388 From the raw VCF files SNP positions containing heterozygous labels were extracted using
389 GATK VariantFiltration. From the 3.3 millions of heterozygous SNPs extracted, two filtering
390 steps were then applied. Only SNPs with a frequency of at least 5% of the population and
391 located in TAIR10-annotated coding regions were kept. After those filtering steps a core set of
392 26647 SNPs were retained for further analysis (**see Supplemental Figure 3**). Gene names
393 and features containing those pseudo-SNPs were extracted from the TAIR10 annotation.

394 GWAS

395 The presence and absence of pseudo-heterozygosity (coded as 1 and 0 respectively) was used
396 as a phenotype to run GWAS. As a genotype the matrix published by the 1001 Genomes
397 Consortium containing 10 million SNPs was been used (1001 Genomes Consortium 2016). To
398 run all the GWAS, the pygwas package (<https://github.com/timeu/PyGWAS>) with the amm
399 (accelerated mixed model) option was used. The raw output containing all SNPs was filtered,
400 removing all SNPs with a minor allele frequency below 0.05 and/or a $-\log_{10}(\text{p-value})$ below 4.

401 For each GWAS performed, the p-value as well as the position was used to call the peaks
402 using the Fourier transform function in R (filterFFT), combined with the peak detection function
403 (peakDetection), from the package NucleR 3.13, to automatically retrieve the position of each
404 peak across the genome. From each peak, the highest SNPs within a region of +/- 10kb around
405 the peak center were used (see the example in **Supplemental Figure 17**). Using all 26647
406 SNPs, a summary table was generated with each pseudo-heterozygous SNP and each GWAS
407 peak detected (**Supplemental Data**). This matrix was then used to generate **Figure 2C**,
408 applying thresholds of $-\log_{10}(\text{p-value})$ of 20 and minor allele frequency of 0.1.

409 Confirmation of GWAS results

410 To confirm the detected duplications, a combination of BLAST and synteny was used on the
411 denovo-assembled genome. Only the insertions that segregate in the 6 new genomes were
412 used (398). For each gene, the corresponding sequence from the TAIR10 annotation was
413 located in the target genome using BLAST (**see Supplemental Figure 5**). A threshold of 70%

414 sequence identity as well as 70% of the initial sequence length was used. The presence of a
415 match within 20kb of the predicted peak position was interpreted as confirmation.

416 Gene ontology

417 Out of the 2570 genes detected to be duplicated, 2396 have a gene ontology annotation.
418 PLAZA.4 (Van Bel et al. 2018) was used to perform a gene enrichment analysis using the full
419 genome as background. Data were then retrieved and plotted using R.

420 Coverage and Methylation analysis

421 Bisulfite reads for the accessions were taken from 1001 methylomes (Kawakatsu et al. 2016).
422 Reads were mapped to PacBio genomes using an nf-core pipeline
423 (<https://github.com/rbpisupati/methylseq>). We filtered for cytosines with a minimum depth of 3.
424 They methylation levels were calculated either on the gene-body or on 200bp windows using
425 custom python scripts following guidelines from Schultz et al. (2012). Weighted methylation
426 levels were used, i.e. if there are three cytosines with a depth of t1, t2 and t3 and number of
427 methylated reads are c1, c2 and c3, the methylation level was calculated as
428 $(c1+c2+c3)/(t1+t2+t3)$. We called a gene “differentially methylated” if the difference in weighted
429 methylation level was more than 0.05 for CG and 0.03 for CHG.

430 The sequencing coverage for each accession was extracted using the function
431 bamCoverage (windows size of 50bp) from the program DeepTools (Ramírez et al. 2016). The
432 Bigwig files generated were then processed in R using the package rtracklayer. No correlation
433 between the mean sequencing coverage and the number of pseudo-SNPs detected was
434 observed (**Supplemental Figure 18**).

435 Multiple sequence alignment

436 For each insertion of the AT1G20390-AT1G20400 (Transposon+gene) fragment, a fasta file
437 including 2kb on each side of the fragment was extracted from each genome, using the getfasta
438 function from bedtools (Quinlan and Hall 2010). Multiple alignment was performed using
439 KALIGN (Madeira et al. 2019). Visualization and comparison was done using Jalview 2
440 (Waterhouse et al. 2009).

441 Structural variation analysis

442 To control the structure of the region around duplicated genes, the sequence from 3 genes
443 upstream and downstream of the gene of interest was extracted. Each sequence was then
444 BLAST to each of the genomes and the position of each BLAST result was retrieved. NCBI
445 BLAST (Altschul et al. 1990) was used with a percentage of identity threshold of 70% and all
446 other parameters as default. From each blast results fragments with at least 50% of the input
447 sequence length have been selected and plotted using R.

448 Frequency of the insertions in the 1001 Genomes dataset

449 The same sequences used for the multiple alignment were used to confirm presence or
450 absence of each insertion in the 1001 Genomes dataset. We used each of those sequences as
451 reference to map short reads using minimap 2 (H. Li 2018). For each insertion, only paired-end
452 reads having both members of the pair mapping to the region were retained. An insertion was
453 considered present in an accession if at least 3 pairs of reads spanned the insertion border (**see**
454 **Supplemental Figure 11**).

455 Multiple species comparison

456 We used the *Capsella rubella* and *A.arenosa* genomes (Slotte et al. 2013; Burns et al. 2021) to
457 search for the new Transposon+gene element, just like in the *A. thaliana* genomes. For *A.*
458 *arenosa* we used the subgenome of *A. suecica*. We located the transposon+gene fragments,
459 extracted from the TAIR10 annotation, using NCBI BLAST as above. For *A.lyrata* two newly
460 assembled genomes were assembled using MinION sequencing.

461 Additional files

462 Additional file 1.txt

463 Methylation value per gene of all accessions mapped to the reference genome

464 CG and CHG weighted average per genes of the 6 accessions analyzed. Row names
465 correspond to the gene ID and column name to the CG and CHG for each accession.

466 Additional file 2-8.csv

467 Methylation value per gene of all accessions mapped to the corresponding genome.

468 CG and CHG weighted average per genes of the 6 accessions analyzed. Row names
469 correspond to the gene ID. (the “_” corresponds to the multiple copies detected). The column
470 name to the CG and CHG for each accession.

471 Acknowledgment

472 We thank numerous people on Twitter for providing feedback on the bioRxiv version.

473 Authors' contributions

474 BJ and MN developed the project. BJ performed all analyses. LMS and RB assembled the
475 *A.thaliana* and *A.lyrata* genomes, respectively. FR generated the SNP matrix. RP performed the
476 methylation analyses. BJ and MN wrote the manuscript, with input from all authors.

477 Funding

478 This project received funding from the European Research Council (ERC) under the European
479 Union's Horizon 2020 research and innovation programme (grant agreement No 789037)

480 Availability of data and materials

481 All genome assemblies and raw reads were deposited under the BioProject ID: PRJNA779205.

482 Link of the genome files for the reviewers:

483 <https://dataview.ncbi.nlm.nih.gov/object/PRJNA779205?>

484 [reviewer=gduvs00c97i3bd5he06gs25oos](https://dataview.ncbi.nlm.nih.gov/object/PRJNA779205?viewer=gduvs00c97i3bd5he06gs25oos)

485 Scripts used are available under Github link: <https://github.com/benjj212/duplication-paper.git>.

486 The full GWAS matrix is available at <https://doi.org/10.5281/zenodo.5702395>

487 Ethics approval and consent to participate

488 Not applicable.

489 Competing interests

490 The authors declare no competing interests.

491 Author details

492 1 Gregor Mendel Institute, Austrian Academy of Sciences, Vienna Biocenter, Vienna, Austria. 2
493 Max Planck Institute for Developmental Biology, Tübingen, Germany. 3 Department of Plant
494 Sciences, University of Cambridge, Cambridge, UK.

495 References

- 496 1001 Genomes Consortium. 2016. “1,135 Genomes Reveal the Global Pattern of Polymorphism
497 in *Arabidopsis Thaliana*.” *Cell* 166 (2): 481–91.
- 498 Alkan, Can, Bradley P. Coe, and Evan E. Eichler. 2011. “Genome Structural Variation Discovery
499 and Genotyping.” *Nature Reviews. Genetics* 12 (5): 363–76.
- 500 Alonge, Michael, Sebastian Soyk, Srividya Ramakrishnan, Xingang Wang, Sara Goodwin, Fritz
501 J. Sedlazeck, Zachary B. Lippman, and Michael C. Schatz. 2019. “RaGOO: Fast and
502 Accurate Reference-Guided Scaffolding of Draft Genomes.” *Genome Biology* 20 (1): 224.
- 503 Alonge, Michael, Xingang Wang, Matthias Benoit, Sebastian Soyk, Lara Pereira, Lei Zhang,
504 Hamsini Suresh, et al. 2020. “Major Impacts of Widespread Structural Variation on Gene
505 Expression and Crop Improvement in Tomato.” *Cell*.
506 <https://doi.org/10.1016/j.cell.2020.05.021>.
- 507 Altschul, S. F., W. Gish, W. Miller, E. W. Myers, and D. J. Lipman. 1990. “Basic Local Alignment
508 Search Tool.” *Journal of Molecular Biology* 215 (3): 403–10.
- 509 Arabidopsis Genome Initiative. 2000. “Analysis of the Genome Sequence of the Flowering Plant

- 510 *Arabidopsis Thaliana*.” *Nature* 408 (6814): 796–815.
- 511 Bukowski, Robert, Xiaosen Guo, Yanli Lu, Cheng Zou, Bing He, Zhengqin Rong, Bo Wang, et
512 al. 2018. “Construction of the Third-Generation Zea Mays Haplotype Map.” *GigaScience* 7
513 (4): 1–12.
- 514 Burns, Robin, Terezie Mandáková, Joanna Gunis, Luz Mayela Soto-Jiménez, Chang Liu, Martin
515 A. Lysak, Polina Yu Novikova, and Magnus Nordborg. 2021. “Gradual Evolution of
516 Allopolyploidy in *Arabidopsis Suecica*.” *Nature Ecology & Evolution* 5 (10): 1367–81.
- 517 Cao, Jun, Korbinian Schneeberger, Stephan Ossowski, Torsten Günther, Sebastian Bender,
518 Joffrey Fitz, Daniel Koenig, et al. 2011. “Whole-Genome Sequencing of Multiple
519 *Arabidopsis Thaliana* Populations.” *Nature Genetics* 43 (10): 956–63.
- 520 Carter, Nigel P. 2007. “Methods and Strategies for Analyzing Copy Number Variation Using
521 DNA Microarrays.” *Nature Genetics* 39 (7 Suppl): S16–21.
- 522 Chia, Jer-Ming, Chi Song, Peter J. Bradbury, Denise Costich, Natalia de Leon, John Doebley,
523 Robert J. Elshire, et al. 2012. “Maize HapMap2 Identifies Extant Variation from a Genome
524 in Flux.” *Nature Genetics* 44 (7): 803–7.
- 525 Cristina Barragan, A., Maximilian Collenberg, Rebecca Schwab, Merijn Kerstens, Ilya Bezrukov,
526 Felix Bemm, Doubravka Požárová, Filip Kolář, and Detlef Weigel. 2021. “Homozygosity at
527 Its Limit: Inbreeding Depression in Wild *Arabidopsis Arenosa* Populations.” *bioRxiv*.
528 <https://doi.org/10.1101/2021.01.24.427284>.
- 529 DePristo, Mark A., Eric Banks, Ryan Poplin, Kiran V. Garimella, Jared R. Maguire, Christopher
530 Hartl, Anthony A. Philippakis, et al. 2011. “A Framework for Variation Discovery and
531 Genotyping Using next-Generation DNA Sequencing Data.” *Nature Genetics* 43 (5): 491–
532 98.
- 533 Gan, Xiangchao, Oliver Stegle, Jonas Behr, Joshua G. Steffen, Philipp Drewe, Katie L.
534 Hildebrand, Rune Lyngsoe, et al. 2011. “Multiple Reference Genomes and Transcriptomes
535 for *Arabidopsis Thaliana*.” *Nature* 477 (7365): 419–23.
- 536 Göktay, Mehmet, Andrea Fulgione, and Angela M. Hancock. 2020. “A New Catalogue of
537 Structural Variants in 1301 *A. Thaliana* Lines from Africa, Eurasia and North America
538 Reveals a Signature of Balancing at Defense Response Genes.” *Molecular Biology and
539 Evolution*, November. <https://doi.org/10.1093/molbev/msaa309>.
- 540 Gonzalez, Enrique, Hemant Kulkarni, Hector Bolivar, Andrea Mangano, Racquel Sanchez,
541 Gabriel Catano, Robert J. Nibbs, et al. 2005. “The Influence of CCL3L1 Gene-Containing
542 Segmental Duplications on HIV-1/AIDS Susceptibility.” *Science* 307 (5714): 1434–40.
- 543 Griffin, P. C., and Y. Willi. 2014. “Evolutionary Shifts to Self-Fertilisation Restricted to

- 544 Geographic Range Margins in North American *Arabidopsis Lyrata*.” *Ecology Letters* 17 (4):
545 484–90.
- 546 Handsaker, Robert E., Joshua M. Korn, James Nemesh, and Steven A. McCarroll. 2011.
547 “Discovery and Genotyping of Genome Structural Polymorphism by Sequencing on a
548 Population Scale.” *Nature Genetics* 43 (3): 269–76.
- 549 Horton, Matthew W., Angela M. Hancock, Yu S. Huang, Christopher Toomajian, Susanna
550 Atwell, Adam Auton, N. Wayan Mulyati, et al. 2012. “Genome-Wide Patterns of Genetic
551 Variation in Worldwide *Arabidopsis Thaliana* Accessions from the RegMap Panel.” *Nature*
552 *Genetics* 44 (2): 212–16.
- 553 Hufford, Matthew B., Arun S. Seetharam, Margaret R. Woodhouse, Kapeel M. Chougule,
554 Shujun Ou, Jianing Liu, William A. Ricci, et al. 2021. “De Novo Assembly, Annotation, and
555 Comparative Analysis of 26 Diverse Maize Genomes.” *Cold Spring Harbor Laboratory*.
556 <https://doi.org/10.1101/2021.01.14.426684>.
- 557 Hurles, Matthew. 2002. “Are 100,000 ‘SNPs’ Useless?” *Science*.
- 558 Hu, Tina T., Pedro Pattyn, Erica G. Bakker, Jun Cao, Jan-Fang Cheng, Richard M. Clark, Noah
559 Fahlgren, et al. 2011. “The *Arabidopsis Lyrata* Genome Sequence and the Basis of Rapid
560 Genome Size Change.” *Nature Genetics* 43 (5): 476–81.
- 561 Jiao, Wen-Biao, and Korbinian Schneeberger. 2019. “Chromosome-Level Assemblies of
562 Multiple *Arabidopsis Thaliana* Accessions Reveal Hotspots of Genomic Rearrangements.”
563 *bioRxiv*. <https://doi.org/10.1101/738880>.
- 564 Kawakatsu, Taiji, Shao-Shan Carol Huang, Florian Jupe, Eriko Sasaki, Robert J. Schmitz, Mark
565 A. Urich, Rosa Castanon, et al. 2016. “Epigenomic Diversity in a Global Collection of
566 *Arabidopsis Thaliana* Accessions.” *Cell* 166 (2): 492–505.
- 567 Koren, Sergey, Brian P. Walenz, Konstantin Berlin, Jason R. Miller, Nicholas H. Bergman, and
568 Adam M. Phillippy. 2017. “Canu: Scalable and Accurate Long-Read Assembly via Adaptive
569 K-Mer Weighting and Repeat Separation.” *Genome Research* 27 (5): 722–36.
- 570 Li, Changsheng, Xiaoli Xiang, Yongcai Huang, Yong Zhou, Dong An, Jiaqiang Dong, Chenxi
571 Zhao, et al. 2020. “Long-Read Sequencing Reveals Genomic Structural Variations That
572 Underlie Creation of Quality Protein Maize.” *Nature Communications* 11 (1): 17.
- 573 Li, Heng. 2013. “Aligning Sequence Reads, Clone Sequences and Assembly Contigs with BWA-
574 MEM.” *arXiv [q-bio.GN]*. arXiv. <http://arxiv.org/abs/1303.3997>.
- 575 ———. 2018. “Minimap2: Pairwise Alignment for Nucleotide Sequences.” *Bioinformatics* 34
576 (18): 3094–3100.
- 577 Li, Heng, Bob Handsaker, Alec Wysoker, Tim Fennell, Jue Ruan, Nils Homer, Gabor Marth,

- 578 Goncalo Abecasis, Richard Durbin, and 1000 Genome Project Data Processing Subgroup.
579 2009. "The Sequence Alignment/Map Format and SAMtools." *Bioinformatics* 25 (16):
580 2078–79.
- 581 Lin, Ke, Ningwen Zhang, Edouard I. Severing, Harm Nijveen, Feng Cheng, Richard G. F.
582 Visser, Xiaowu Wang, Dick de Ridder, and Guusje Bonnema. 2014. "Beyond Genomic
583 Variation - Comparison and Functional Annotation of Three Brassica Rapagenomes: A
584 Turnip, a Rapid Cycling and a Chinese Cabbage." *BMC Genomics* 15 (1): 250.
- 585 Lisch, Damon. 2013. "How Important Are Transposons for Plant Evolution?" *Nature Reviews*.
586 *Genetics* 14 (1): 49–61.
- 587 Liu, Dong-Xu, Ramesh Rajaby, Lu-Lu Wei, Lei Zhang, Zhi-Quan Yang, Qing-Yong Yang, and
588 Wing-Kin Sung. 2021. "Calling Large Indels in 1047 Arabidopsis with IndelEnsembler."
589 *Nucleic Acids Research*, October. <https://doi.org/10.1093/nar/gkab904>.
- 590 Liu, Yucheng, Huilong Du, Pengcheng Li, Yanting Shen, Hua Peng, Shulin Liu, Guo-An Zhou, et
591 al. 2020. "Pan-Genome of Wild and Cultivated Soybeans." *Cell*, June.
592 <https://doi.org/10.1016/j.cell.2020.05.023>.
- 593 Long, Quan, Fernando A. Rabanal, Dazhe Meng, Christian D. Huber, Ashley Farlow, Alexander
594 Platzer, Qingrun Zhang, et al. 2013. "Massive Genomic Variation and Strong Selection in
595 Arabidopsis Thaliana Lines from Sweden." *Nature Genetics* 45 (8): 884–90.
- 596 Lu, Fei, Maria C. Romay, Jeffrey C. Glaubitz, Peter J. Bradbury, Robert J. Elshire, Tianyu
597 Wang, Yu Li, et al. 2015. "High-Resolution Genetic Mapping of Maize Pan-Genome
598 Sequence Anchors." *Nature Communications* 6 (April): 6914.
- 599 Madeira, Fábio, Young Mi Park, Joon Lee, Nicola Buso, Tamer Gur, Nandana Madhusoodanan,
600 Prasad Basutkar, et al. 2019. "The EMBL-EBI Search and Sequence Analysis Tools APIs in
601 2019." *Nucleic Acids Research* 47 (W1): W636–41.
- 602 Martin, Marcel. 2011. "Cutadapt Removes Adapter Sequences from High-Throughput
603 Sequencing Reads." *EMBnet.journal* 17 (1): 10–12.
- 604 Melquist, S., B. Luff, and J. Bender. 1999. "Arabidopsis PAI Gene Arrangements, Cytosine
605 Methylation and Expression." *Genetics* 153 (1): 401–13.
- 606 Miyahara, E., J. Pokorny, V. C. Smith, R. Baron, and E. Baron. 1998. "Color Vision in Two
607 Observers with Highly Biased LWS/MWS Cone Ratios." *Vision Research* 38 (4): 601–12.
- 608 Morgante, Michele, Stephan Brunner, Giorgio Pea, Kevin Fengler, Andrea Zuccolo, and Antoni
609 Rafalski. 2005. "Gene Duplication and Exon Shuffling by Helitron-like Transposons
610 Generate Intraspecies Diversity in Maize." *Nature Genetics* 37 (9): 997–1002.
- 611 Perry, George H., Nathaniel J. Dominy, Katrina G. Claw, Arthur S. Lee, Heike Fiegler, Richard

- 612 Redon, John Werner, et al. 2007. "Diet and the Evolution of Human Amylase Gene Copy
613 Number Variation." *Nature Genetics* 39 (10): 1256–60.
- 614 Pinosio, Sara, Stefania Giacomello, Patricia Faivre-Rampant, Gail Taylor, Veronique Jorge,
615 Marie Christine Le Paslier, Giusi Zaina, et al. 2016. "Characterization of the Poplar Pan-
616 Genome by Genome-Wide Identification of Structural Variation." *Molecular Biology and*
617 *Evolution* 33 (10): 2706–19.
- 618 Purcell, Shaun, Benjamin Neale, Kathe Todd-Brown, Lori Thomas, Manuel A. R. Ferreira, David
619 Bender, Julian Maller, et al. 2007. "PLINK: A Tool Set for Whole-Genome Association and
620 Population-Based Linkage Analyses." *American Journal of Human Genetics* 81 (3): 559–
621 75.
- 622 Quadrana, Leandro, Amanda Bortolini Silveira, George F. Mayhew, Chantal LeBlanc, Robert A.
623 Martienssen, Jeffrey A. Jeddloh, Vincent Colot, and Daniel Zilberman. 2016. "The
624 Arabidopsis Thaliana Mobilome and Its Impact at the Species Level." *eLife* 5 (June):
625 e15716.
- 626 Quinlan, Aaron R., and Ira M. Hall. 2010. "BEDTools: A Flexible Suite of Utilities for Comparing
627 Genomic Features." *Bioinformatics* 26 (6): 841–42.
- 628 Ramírez, Fidel, Devon P. Ryan, Björn Grüning, Vivek Bhardwaj, Fabian Kilpert, Andreas S.
629 Richter, Steffen Heyne, Friederike Dünder, and Thomas Manke. 2016. "deepTools2: A next
630 Generation Web Server for Deep-Sequencing Data Analysis." *Nucleic Acids Research* 44
631 (W1): W160–65.
- 632 Ranade, K., M. S. Chang, C. T. Ting, D. Pei, C. F. Hsiao, M. Olivier, R. Pesich, et al. 2001.
633 "High-Throughput Genotyping with Single Nucleotide Polymorphisms." *Genome Research*
634 11 (7): 1262–68.
- 635 Schneeberger, Korbinian, Stephan Ossowski, Felix Ott, Juliane D. Klein, Xi Wang, Christa Lanz,
636 Lisa M. Smith, et al. 2011. "Reference-Guided Assembly of Four Diverse Arabidopsis
637 Thaliana Genomes." *Proceedings of the National Academy of Sciences of the United*
638 *States of America* 108 (25): 10249–54.
- 639 Schultz, Matthew D., Robert J. Schmitz, and Joseph R. Ecker. 2012. "'Leveling' the Playing
640 Field for Analyses of Single-Base Resolution DNA Methylomes." *Trends in Genetics: TIG*
641 28 (12): 583–85.
- 642 Sedlazeck, Fritz J., Philipp Rescheneder, Moritz Smolka, Han Fang, Maria Nattestad, Arndt von
643 Haeseler, and Michael C. Schatz. 2018. "Accurate Detection of Complex Structural
644 Variations Using Single-Molecule Sequencing." *Nature Methods* 15 (6): 461–68.
- 645 Shendure, Jay, and Hanlee Ji. 2008. "Next-Generation DNA Sequencing." *Nature Biotechnology*

- 646 26 (10): 1135–45.
- 647 Slotte, Tanja, Khaled M. Hazzouri, J. Arvid Ågren, Daniel Koenig, Florian Maumus, Ya-Long
648 Guo, Kim Steige, et al. 2013. “The Capsella Rubella Genome and the Genomic
649 Consequences of Rapid Mating System Evolution.” *Nature Genetics* 45 (7): 831–35.
- 650 Snijders, A. M., N. Nowak, R. Seagraves, S. Blackwood, N. Brown, J. Conroy, G. Hamilton, et al.
651 2001. “Assembly of Microarrays for Genome-Wide Measurement of DNA Copy Number.”
652 *Nature Genetics* 29 (3): 263–64.
- 653 Stritt, Christoph, Elena L. Gimmi, Michele Wyler, Abdelmonaim H. Bakali, Aleksandra Skalska,
654 Robert Hasterok, Luis A. J. Mur, Nicola Pecchioni, and Anne C. Roulin. 2021. “Migration
655 without Interbreeding: Evolutionary History of a Highly Selfing Mediterranean Grass Inferred
656 from Whole Genomes.” *Molecular Ecology*, October. <https://doi.org/10.1111/mec.16207>.
- 657 Sun, Hequan, Jia Ding, Mathieu Piednoël, and Korbinian Schneeberger. 2018. “findGSE:
658 Estimating Genome Size Variation within Human and Arabidopsis Using K-Mer
659 Frequencies.” *Bioinformatics* 34 (4): 550–57.
- 660 Tarasov, Artem, Albert J. Vilella, Edwin Cuppen, Isaac J. Nijman, and Pjotr Prins. 2015.
661 “Sambamba: Fast Processing of NGS Alignment Formats.” *Bioinformatics* 31 (12): 2032–
662 34.
- 663 Van Bel, Michiel, Tim Diels, Emmelien Vancaester, Lukasz Kreft, Alexander Botzki, Yves Van
664 de Peer, Frederik Coppens, and Klaas Vandepoele. 2018. “PLAZA 4.0: An Integrative
665 Resource for Functional, Evolutionary and Comparative Plant Genomics.” *Nucleic Acids
666 Research* 46 (D1): D1190–96.
- 667 Van der Auwera, Geraldine A., Mauricio O. Carneiro, Chris Hartl, Ryan Poplin, Guillermo Del
668 Angel, Ami Levy-Moonshine, Tadeusz Jordan, et al. 2013. “From FastQ Data to High
669 Confidence Variant Calls: The Genome Analysis Toolkit Best Practices Pipeline.” *Current
670 Protocols in Bioinformatics / Editorial Board, Andreas D. Baxevanis ... [et Al.]* 11 (1110):
671 11.10.1–11.10.33.
- 672 Vaser, Robert, Ivan Sović, Niranjana Nagarajan, and Mile Šikić. 2017. “Fast and Accurate de
673 Novo Genome Assembly from Long Uncorrected Reads.” *Genome Research* 27 (5): 737–
674 46.
- 675 Walker, Bruce J., Thomas Abeel, Terrance Shea, Margaret Priest, Amr Abouelliel, Sharadha
676 Sakthikumar, Christina A. Cuomo, et al. 2014. “Pilon: An Integrated Tool for
677 Comprehensive Microbial Variant Detection and Genome Assembly Improvement.” *PloS
678 One* 9 (11): e112963.
- 679 Waterhouse, Andrew M., James B. Procter, David M. A. Martin, Michèle Clamp, and Geoffrey J.

- 680 Barton. 2009. "Jalview Version 2--a Multiple Sequence Alignment Editor and Analysis
681 Workbench." *Bioinformatics* 25 (9): 1189–91.
- 682 Woodhouse, Margaret R., Brent Pedersen, and Michael Freeling. 2010. "Transposed Genes in
683 Arabidopsis Are Often Associated with Flanking Repeats." *PLoS Genetics* 6 (5): e1000949.
- 684 Yao, Wen, Guangwei Li, Hu Zhao, Gongwei Wang, Xingming Lian, and Weibo Xie. 2015.
685 "Exploring the Rice Dispensable Genome Using a Metagenome-like Assembly Strategy."
686 *Genome Biology* 16 (September): 187.
- 687 Zhao, Min, Qingguo Wang, Quan Wang, Peilin Jia, and Zhongming Zhao. 2013. "Computational
688 Tools for Copy Number Variation (CNV) Detection Using next-Generation Sequencing
689 Data: Features and Perspectives." *BMC Bioinformatics* 14 Suppl 11 (September): S1.
- 690 Zhou, Yong, Dmytro Chebotarov, Dave Kudrna, Victor Llaca, Seunghee Lee, Shanmugam
691 Rajasekar, Nahed Mohammed, et al. 2020. "A Platinum Standard Pan-Genome Resource
692 That Represents the Population Structure of Asian Rice." *Scientific Data* 7 (1): 113.
- 693 Zmienko, Agnieszka, Malgorzata Marszalek-Zenczak, Pawel Wojciechowski, Anna Samelak-
694 Czajka, Magdalena Luczak, Piotr Kozlowski, Wojciech M. Karlowski, and Marek
695 Figlerowicz. 2020. "AthCNV: A Map of DNA Copy Number Variations in the Arabidopsis
696 Genome." *The Plant Cell* 32 (6): 1797–1819.